^{87}Rb nuclear magnetic resonance evidence for solitons and phasons in Rb_2ZnBr_4

V. Rutar, F. Milia,* B. Topič, and R. Blinc
J. Stefan Institute, E. Kardelj University of Ljubljana, Ljubljana, Yugoslavia

Th. Rasing
Research Institute for Materials, University of Nijmegen, Toernooiveld, 6525 ED Nijmegen, The Netherlands

(Received 18 June 1981)

The temperature and angular dependences of the ^{87}Rb $\frac{1}{2} \rightarrow -\frac{1}{2}$ NMR spectra and spin-lattice relaxation times have been studied in the paraelectric (*P*), the incommensurate (*I*), and the ferroelectric commensurate (*C*) phases of Rb_2ZnBr_4, and the distributions of the electric-field-gradient (EFG) tensors at the Rb sites have been determined in the *P* and *I* phases. The NMR line shapes can be described by "broad solitons" over most of the *I* phase whereas the soliton width becomes small as compared to the intersoliton distance close to the transition into the *C* phase. The temperature dependence of the soliton density has been determined. The spin-lattice relaxation rate in the *I* phase is dominated by phasons if the nuclear displacement is small, whereas it is dominated by amplitudons if the nuclear displacement from the paraelectric site is large. Soliton pinning by defects has been confirmed.

I. INTRODUCTION

Incommensurate (*I*) systems have attracted a great deal of attention in the last few years.[1,2] They are characterized by the appearance of a superlattice with a periodicity which is an irrational fraction of the periodicity of the basic lattice.

Rb_2ZnBr_4 represents one of the first known examples of one-dimensionally modulated incommensurate systems.[3–5] It undergoes successive phase transitions at $T_I = 346$ K and $T_c = 187$ K.[6] The high-temperature space group is D_{2h}^{16}-*Pcmn* and the low-temperature space group is C_{2v}^{9}-$Pc2_1n$. When it is cooled through T_I the crystal exhibits an instability against a soft mode which condenses out at a general point in the Brillouin zone. The order parameter of such a transition

$$u = A\cos\phi(z) \tag{1}$$

is characterized by its amplitude A and its phase $\phi(z)$. Mc Millan[7] has proposed that the *I* phase actually consists of commensurate regions [$\phi(z)$=const] separated by solitonlike "discommensurations" where the phase changes rapidly. Many attempts have been made to use this concept in explaining various experimental results.[8–17] Advanced NMR (Ref. 15) and nuclear quadrupole resonance[16] (NQR) studies have shown that in the isomorphic Rb_2ZnCl_4 solitons are narrow only close to the lock-in transition ($T_c < T < T_c + \sim 10$ K), while in the bulk of the *I* phase they are broad compared with the intersoliton distance and can be suitable described by the "plane-wave" limit. The same picture was proposed for K_2SeO_4 on the basis of ultrasonic measurements of the shear stiffness c_{55}.[17]

The ^{87}Rb NMR measurements of Rb_2ZnCl_4 (Refs. 11 and 18) and Rb_2ZnBr_4 (Ref. 12) demonstrated that the Rb nucleus is very suitable for the study of the local structure and the dynamics of the *I* phase. In the present paper we present a detailed study of the incommensurate modulation in Rb_2ZnBr_4. Experimental details are described in Sec. II. ^{87}Rb electric field gradient (EFG) tensors in the paraelectric (*P*) and the incommensurate (*I*) phase are reported in Sec. III, while the temperature dependence of the spectra is analyzed in Sec. IV. The temperature dependence of the soliton density is reported in Sec. V together with a discussion of the large thermal hysteresis at the lock-in transition. Section VI describes the "incommensurate" line shape and spin-lattice relaxation around T_I. The phason and the amplitudon contributions to the relaxation rate are reported in Sec. VII.

II. EXPERIMENTAL

A single crystal of Rb_2ZnBr_4 was grown at 303 K from an aqueous solution of RbBr and $ZnBr_2$ in a 2:1 molar ratio. The crystal was colorless though not completely transparent. The orientation of the crystallographic axes has been determined from its morphology and was further checked by x-ray diffraction.

The NMR measurements of the ^{87}Rb ($I=\frac{3}{2}$) line shapes and relaxation times have been done on the Bruker SXP spectrometer. The ^{87}Rb satellites ($\frac{3}{2}\rightarrow\frac{1}{2}$ and $-\frac{1}{2}\rightarrow-\frac{3}{2}$) are to broad to be observed in the I phase, therefore only the central lines ($\frac{1}{2}\rightarrow-\frac{1}{2}$) were studied. Since second-order quadrupolar shifts are inversely proportional to the Larmor frequency (ν_L), a part of the spectra were taken at $\nu_L=29.5$ MHz on the iron magnet ($B_0=2.1$ T) to obtain better resolution, while a superconducting magnet ($B_0=6.3$ T, $\nu_I=88.3$ MHz) was used for most of the spin-lattice relaxation-time measurements. The 180°-t-90°-τ-180° pulse sequence has been used.

III. EFG TENSORS IN THE I PHASE

Expanding the μth component $V^{(\mu)}(l)$ of the EFG tensor at the lth lattice site in powers of the nuclear displacements around the values $V_0^{(\mu)}(l)$ corresponding to the average structure of the P phase and assuming that the wavelength of the incommensurate modulation is large compared with the radius of the region where the dominant contribution to the EFG tensor comes from, we find[19]

$$V^{(\mu)}(l)=V_0^{(\mu)}(l)+A\cos\phi(z)V_{01}^{(\mu)}(l)+A^2\cos^2\phi(z)V_{02}^{(\mu)}(l)+\cdots, \quad (2)$$

where $V_{01}^{(\mu)}(l)$ and $V_{02}^{(\mu)}(l)$ are constants. Since $\cos\phi(z)$ is continuous in the I phase, we expect a quasicontinuous distribution of the EFG tensor components in the interval

$$V_{\pm}^{(\mu)}(l)=V_0^{(\mu)}(l)\pm AV_{01}^{(\mu)}(l)+A^2V_{02}^{(\mu)}(l)\pm\cdots. \quad (3)$$

The limiting values $V_{\pm}^{(\mu)}(l)$ correspond to nuclei which are near the maximum positive or negative displacements. These values were determined by measuring the angular dependence of those central $\frac{1}{2}\rightarrow-\frac{1}{2}$ transitions which correspond to the edge singularities in the frequency distribution $f(\nu)$. The results have been analyzed by the method of Volkoff.[20]

The paraelectric unit cell contains eight Rb ions which can be divided into two chemically inequivalent sets, Rb(1) and Rb(2). All Rb sites have site symmetry m.[21] Because of the presence of the center of symmetry at most two Rb sites can be distinguished for each chemically inequivalent set. We thus expect to see at most four Rb lines for $T>T_I$. For a general direction of the magnetic field in the (a-c) plane all four lines should be seen whereas only two lines should be seen in the (a-b) and (b-c) planes. In view of the Rb site symmetry, the EFG tensor components V_{ba} and V_{bc} should vanish for $T>T_I$ and one of the principal axes should be parallel to the crystal b axis which becomes the axis of spontaneous polarization below T_c.[19,22]

The experimental data (Fig. 1 and Table I) agree very well with the predictions based on the crystal structure. We find two chemically inequivalent Rb sites. Each of them occurs in two different orientations generated by the c mirror. The quadrupole coupling constants equal $e^2qQ/H=4.5$ MHz for Rb(1) and $e^2qQ/h=3.0$ MHz for Rb(2). The corresponding asymmetry parameters are $\eta=0.87$ and $\eta=0.57$ (Table II). The principal axes of the Rb(2) EFG tensor coincide with the crystallographic axes within the limits of experimental error ($\pm3°$) and the smallest principal axis points along the b direction. The principal axes of the Rb(1) EFG tensor are, however, rotated with respect to the crystallographic axes for $\pm2.5°$ around the b axis. The largest principal axis is here parallel to the b direction (Table II).

The orientation of the EFG tensors is in good agreement with the results of de Pater[23] whereas our values for the quadrupole coupling constants are significantly lower than his values [Rb(1)↔6.28 MHz and Rb(2)↔ 4.32 MHz]. The reason for this discrepancy is not known.

In view of the a-c mirror plane above T_I the EFG tensor is in the crystal fixed $x||a$, $y||b$, $z||c$ frame of the following

$$V^P=\begin{vmatrix} V_{xx} & 0 & V_{xz} \\ 0 & V_{yy} & 0 \\ V_{xz} & 0 & V_{zz} \end{vmatrix}, \quad T>T_I\,. \quad (4)$$

The frozen-in soft-mode displacements destroy the a-c mirror plane in the I phase resulting in nonzero values of V_{xy} and V_{yz}. We thus expect for a given Rb site the EFG tensor in the I phase to be of the following form:

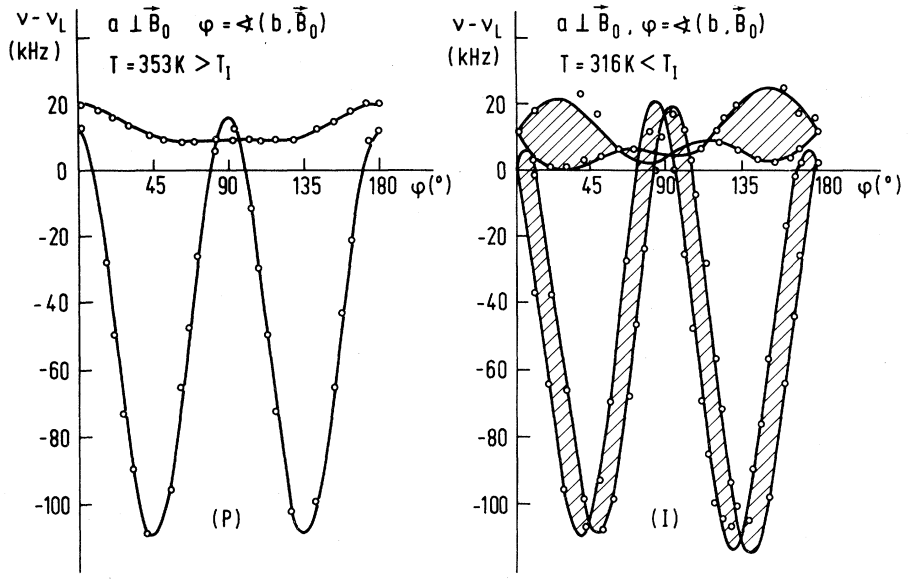

FIG. 1. Angular dependence of second-order quadrupolar shifts in the paraelectric (*P*) and the upper part of the incommensurate (*I*) phase. Hatched regions denote quasicontinuous frequency distributions, limited by edge singularities.

$$V^I = V^P + \begin{vmatrix} 0 & \alpha & 0 \\ \alpha & 0 & \gamma \\ 0 & \gamma & 0 \end{vmatrix} A\cos\phi, \quad T < T_I \tag{5}$$

If only the leading nonzero terms in the expansion of V^I in powers of the incommensurate modulation are considered. Here α and γ are constants and A is the amplitude of the incommensurate order parameter.

As can be seen from Table I this is exactly what happens below T_I. The main effect of the incommensurate phase transition is a rotation of the principal axes of the EFG tensors (Table II) whereas there is only a slight change in the quadrupole coupling constants and asymmetry parameters. For nuclei which are at sites of extreme nuclear displacement of the modulation wave the Rb(2) EFG tansors are at 10 K below T_I rotated for $\pm 19.5°$ around the a and for $\pm 8.7°$ around the c axis whereas the rotation of the Rb(1) EFG tensors amounts to $\pm 8.5°$ around the c and to $\pm 4.5°$ around the b axis. There is a quasicontinuous dis-

TABLE I. ^{87}Rb quadrupole coupling tensors (in MHz) in the crystal fixed a,b,c frame in Rb_2ZnBr_4: (i) $T=353>T_I$, (ii) $T=336$ K $<T_I$, (iii) $T=316$ K $<T_I$. For $T<T_I$ only those tensors are listed which correspond to the extreme displacements of the incommensurate displacement wave.

	Rb(1)			Rb(2)		
$T=353$ K $>T_I$:						
	0.30	0.00	± 0.15	3.00	0.00	0.00
		-4.50	0.00		-0.65	0.00
			4.20			-2.35
$T=336$ K $<T_I=346$ K:						
	0.30	± 0.77	∓ 0.23	3.00	∓ 0.48	∓ 0.23
		-4.50	∓ 0.60		-0.65	± 0.77
			4.20			-2.35
$T=316$ K $<T_I=346$ K:						
	0.30	± 1.10	∓ 0.30	3.00	± 0.71	± 0.36
		-4.50	∓ 0.80		-0.65	± 1.10
			4.20			-2.35

TABLE II. Eigenvalues λ_i (in MHz) and direction cosines of the ^{87}Rb quadrupole coupling tensors in Rb_2ZnBr_4: (i) $T=353$ K $> T_I$, (ii) $T=336$ K $< T_I$. Here again only those tensors are listed for $T<T_I$ which corresponds to the extreme displacements of the incommensurate displacement wave, and the crystallographic axes are chosen according to *Pcmn*: $a=13.343$ Å, $b=7.656$ Å, $c=9.708$ Å.

	$T>T_I$			$T<T_I$		
Rb(1)	$\gamma_1=0.30$	$\gamma_2=4.2$	$\gamma_3=-4.5$	$\gamma_1=0.394$	$\gamma_2=4.262$	$\gamma_3=-4.656$
μ_a	0.9993	$\mp$0.0384	0	0.9860	$\mp$0.0722	$\mp$0.1504
μ_b	0.0000	0.0000	1	$\pm$0.1450	$\mp$0.0750	0.9866
μ_c	$\pm$0.0384	0.9993	0	$\pm$0.0825	0.9946	$\pm$0.629
Rb(2)	$\gamma_1=-0.65$	$\gamma_2=-2.35$	$\gamma_3=3.00$	$\gamma_1=-0.435$	$\gamma_2=-2.647$	$\gamma_3=3.0825$
μ_a	0	0	1	$\mp$0.1526	$\mp$0.0076	0.9882
μ_b	1	0	0	0.9231	$\mp$0.3581	$\pm$0.1480
μ_c	0	1	0	$\pm$0.3529	0.9339	$\pm$0.0624

tribution of EFG tensors between these extremes. The fact that the Rb(2) EFG tensor is more affected than the Rb(1) agrees with the structural data of de Pater.[21]

The rotation angles significantly increase on further cooling into the I phase. At 316 K and the Rb(2) rotation angles increase to $\pm 23°$ around the a and to $\pm 13°$ around the c axis whereas the Rb(1) rotation angles now amount to $\pm 11°$ around the c and to $\pm 6°$ around the b axis. It is as well interesting to note (Fig. 2) that with decreasing temperature the asymmetry parameter η decreases for Rb(1) whereas it increases for Rb(2).

IV. TEMPERATURE DEPENDENCE OF SPECTRA

It has been shown previously[18] that the second-order quadrupolar shift of the frequency of the central ^{87}Rb line can be expanded in a Taylor series in powers of the order parameter

$$\nu=\nu_0(T)+a_1u+\tfrac{1}{2}a_2u^2+\cdots . \tag{6}$$

Here $\nu_0(T)$ denotes the noncritical part of the second-order shift while the parameters $a_1, a_2, a_3, \ldots$ depend on the EFG tensor elements and the orientation of the external magnetic field with respect to the crystal axes. Taking into account that $u=A\cos\phi$ we find

$$\nu=\nu_0(T)+a_1A\cos\phi+\tfrac{1}{2}a_2A^2\cos^2\phi+\cdots . \tag{7}$$

The frequency distribution $f(\nu)$ in the I phase is obtained[18] from

$$f(\nu)d\nu=N(z)dz . \tag{8}$$

As the number of nuclei per unit length in the direction of the modulation $N(z)$ is constant[18] we find

$$f(\nu)=\frac{\text{const}}{|d\nu/dz|} \tag{9}$$

The derivative

$$\frac{d\nu}{dz}=-(a_1A+a_2A^2\cos\phi+\cdots)\sin\phi\frac{d\phi}{dz} \tag{10}$$

therefore describes the shape of the quasicontinuous spectrum in the I phase.[15,16] The frequency distribution is peaked whenever $d\nu/dz=0$.

If the solitons are so broad that the commensurate regions can be neglected,[15] the plane-wave approximation $d\phi/dz=$const is suitable and the derivative (10) becomes

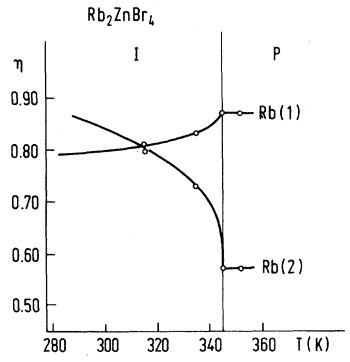

FIG. 2. Temperature dependence of the asymmetry parameters η.

$$\frac{d\nu}{dz} \propto (a_1 A + a_2 A^2 \cos\phi + \cdots)\sin\phi \ . \tag{11}$$

The first possibility

$$\sin\phi = 0 \tag{12}$$

gives rise to singularities

$$\nu_{\pm} = \nu_0 \pm a_1 A + \tfrac{1}{2} a_2 A^2 \pm \cdots \tag{13}$$

which represent signals of nuclei close to the extreme displacements in the incommensurate wave. Their difference

$$\nu_+ - \nu_- = 2a_1 A \propto (T_I - T)^{\beta} \tag{14}$$

is proportional to the amplitude of the order parameter. If we orient the crystal in such a way that higher-order odd terms can be neglected ($a_3 = a_5 = \cdots = 0$), the critical exponent $\beta = 0.35 \pm 0.03$ is obtained by plotting $\nu_+ - \nu_-$ versus $T_I - T$ in a log-log scale (Fig. 3). The obtained value is significantly smaller than the classical mean-field result (0.50), but agrees fairly well with the predictions of the $d=3$, $n=2$ Heisenberg model as well as with neutron scattering experiments on Rb_2ZnBr_4,[4] Rb_2ZnCl_4,[24] and K_2SeO_4.[2] It also agrees with NMR,[15] NQR,[16] EPR,[25] and ultrasonic[26] measurements on these and related compounds.

Additional singularities ($\nu_3, \nu_4, \ldots$) might appear in the spectrum if

$$a_1 A + a_2 A^2 \cos\phi + \cdots = 0 \ . \tag{15}$$

They arise from the nonlinearity in the relation between the frequency and displacements and are shifted for a constant value with respect to $\nu_0(T)$. Since these signals do not depend on A their presence might be used to study the properties of the basic lattice[16] in the I phase.

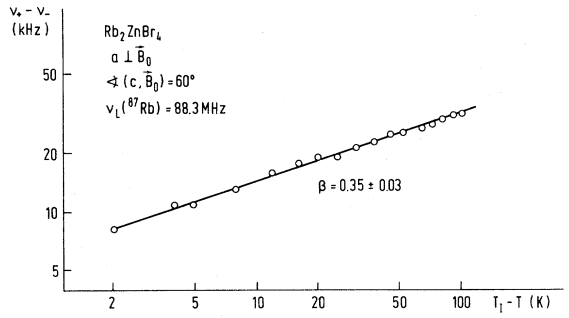

FIG. 3. Log-log plot of the separation between the edge singularities versus $T_I - T$. The value of the exponent $\beta = 0.35 \pm 0.03$ demonstrates that the whole I phase is critical.

V. SOLITON DENSITY

Close to the lock-in transition the distance between the solitons becomes large as compared to the soliton width. The plane-wave approximation no longer accounts for the observed spectrum[15] and the nonlinear spatial variation of $\phi(z)$ must be taken into account. The quantitative theory of the NMR line shape in a multisoliton lattice has been described elsewhere.[27] Since $d\phi(z)/dz \approx 0$ in the commensurate regions, additional "commensurate" peaks start to grow at the position of ferroelectric lines when approaching T_0 (Fig. 4), whereas at the same time the intensity of the "incommensurate" edge singularities decreases. The normalized intensity of the C lines measures the relative volume fraction n_c of commensurate domains. The soliton density (n_s) is equal to

$$n_s = 1 - n_c \ . \tag{16}$$

Our estimate of n_s is not very accurate, since it is affected by several difficulties.

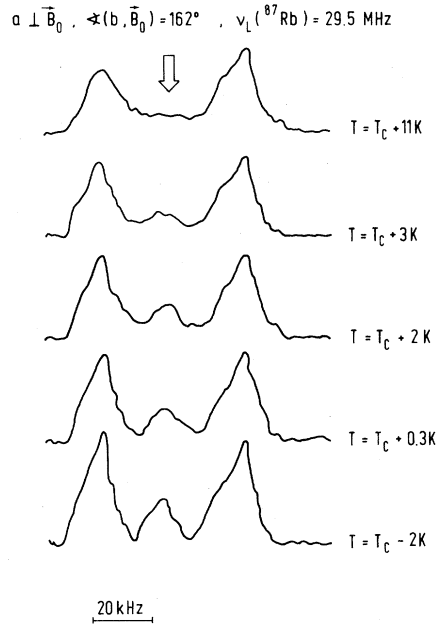

FIG. 4. Temperature dependence of the Rb(2) line shape close to T_c showing the appearance of a commensurate line on formation of a narrow multisoliton lattice. At this orientation the incommensurate edge singularities continue into ferroelectric lines.

(i) The peaks in Rb_2ZnRb_4 are so broad that it is possible to separate commensurate signals from the other singularities only at favorable orientations.

(ii) The spectra were obtained by Fourier transforming spin-echo signals and might be thus distorted by pulse imperfections.

(iii) The spatial variation of the amplitude of the order parameter has been ignored.[28] The results have been found, however, to be reproducible, when measurements were repeated several times under the same experimental conditions.

In Fig. 5 we plotted n_s^2 as a function of temperature. In the temperature interval of $\sim$ 5 K the temperature variation of the soliton density is—as in Rb_2ZnCl_4 (Ref. 15)—consistent with[29,15]

$$n_s \propto (T-T_c)^{1/2} \tag{17}$$

though a logarithmic law[7] cannot be definitely excluded. At higher temperatures saturation sets in and the soliton density is in the middle of the I phase greater than 95%.

The soliton density versus $T-T_c$ curve shows a temperature hysteresis ($\sim$ 10 K), which is considerably larger than in Rb_2ZnCl_4.[15] This is probably due to soliton pinning on defects, as discussed and experimentally demonstrated by Hamano *et al.*[30] It was also noticed that both the transition temperatures T_I and T_c (Refs. 6 and 31) and the undercooling of the I phase[32] are sample dependent. The Rb_2ZnBr_4 crystals used in this study were grown in the I phase, therefore a high concentration of defects is expected. It is possible that the behavior of a sample prepared above T_I will be closer to that of Rb_2ZnCl_4.

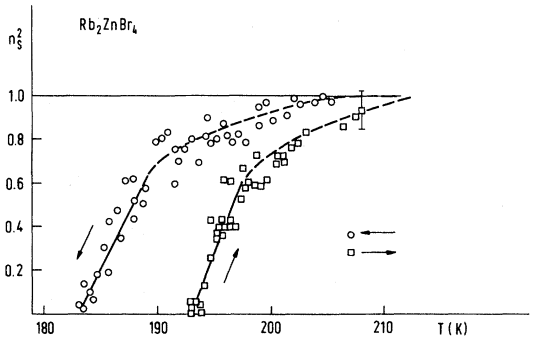

FIG. 5. Square of the soliton density as a function of temperature. In the vicinity of the lock-in transition ($\sim$ 5 K) the temperature variation of the soliton density is consistent with Natterman's prediction (Ref. 29) $n_s \propto (T-T_c)^{0.5}$.

VI. SPECTRA IN THE VICINITY OF T_I

We have found that in Rb_2ZnBr_4 additional lines are observed close to T_I (Fig. 6). They are found at any orientation at exactly the same position as the corresponding paraelectric lines, so that existence of "domains" of the high-temperature phase is indicated.

Since these "paraelectric" lines disappear when the sample is cooled more than $\sim$ 10 K below T_I and since they are not observed in Rb_2ZnCl_4, we conclude that their origin is due to defects which stabilize partial paraelectric arrangements. When the temperature is decreasing away from T_I the stabilizing forces are not strong enough and the incommensurate displacements become dominant.

These lines do not represent signals of macroscopic domains of the undercooled paraelectric phase, because (i) the P-I transition is of the second order, (ii) no thermal hysteresis was observed at T_I, (iii) the spin-lattice relaxation time T_1 (see Fig. 7) of these lines does not follow the paraelectric behavior below T_I, and (iv) the plane-wave model suitably predicts the position of the edge singularities.

Our results demonstrate that the incommensu-

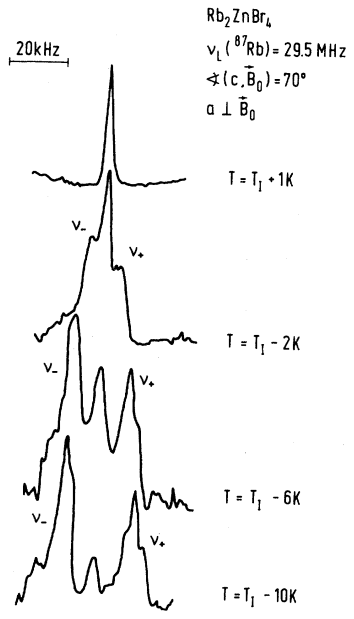

FIG. 6. ^{87}Rb spectra in the vicinity of T_I. Besides the edge singularities ($\nu_\pm$) which are predicted by the plane-wave model, a virtual continuation of the "paraelectric" line is observed for $\sim$ 10 K into the I phase.

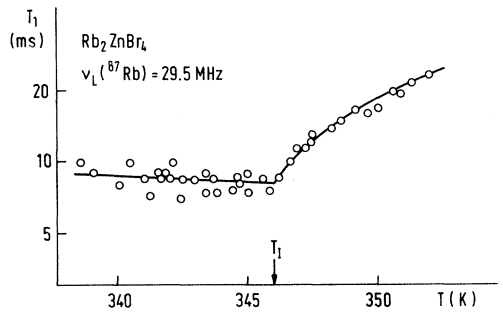

FIG. 7. Temperature dependence of the spin-lattice relaxation time T_1 as measured on the "paraelectric" line near T_I.

rate structure is very subtle and that "defects" must be considered in any complete theoretical description of this phase in "real" crystals.

VII. SPIN-LATTICE RELAXATION TIMES

Since the spin-lattice relaxation times provide additional information about the dynamics of the I phase,[11,18] we decided to extend our previous T_1 measurements.[12] When approaching T_I from above, T_1 rapidly decreases as in other related crystals.[33,34] The relaxation is governed by an overdamped soft mode, which condenses out producing a sharp T_1 minimum at T_I.[35] In the I phase T_1 remains short and nearly temperature independent at the center of the incommensurate frequency distribution (Fig. 8). On the other hand, a normal soft-mode behavior has been observed at the edge singularity close to T_I only, while on further cooling T_1 remains nearly constant till the lock-in transition.

The excitation spectrum of the I phase consists of two modes: the amplitudon branch corresponding to oscillations of the amplitude of the displacement wave and a phason branch reflecting changes of the phase.[36] The last mode—acousticlike mode—has for the critical wave vector zero frequency over whole I phase as it represents only another choice of the phase and therfore needs no excitation energy. In view of its low frequency and large nuclear displacements it represents a very efficient spin-lattice relaxation mechanism. Our measurements have indeed confirmed the presence of such a low-lying, nearly temperature-independent and strong relaxation mechanism. Phasons disappear at T_c where T_1 starts to increase rapidly.

The above statement is further supported by the fact (Fig. 8) that the relaxation time T_1 varies over the spectrum as theoretically predicted.[18,37] At the edge singularities T_1 is significantly longer than in the middle of the broad background. These results fit very well to the theoretical model[37] which predicts that the strong phason contribution dominates the relaxation of the nuclei, which are only slightly displaced ($u \sim 0$), while amplitudons become important for extreme displacements ($u = \pm A$). The phason contribution is temperature independent whereas the amplitudon contributions varies as the amplitude of the order parameter.

The above model is only qualitatively correct as it neglects coupling between phasons and amplitudons as well as the finite width of the resonance signals. Both of these effects result in a mixing of phason and amplitudon contributions.[37]

At a special orientation of the crystal in the magnetic field, an additional minimum was found at $\sim$ 280 K (Fig. 9). Since it is not observed in

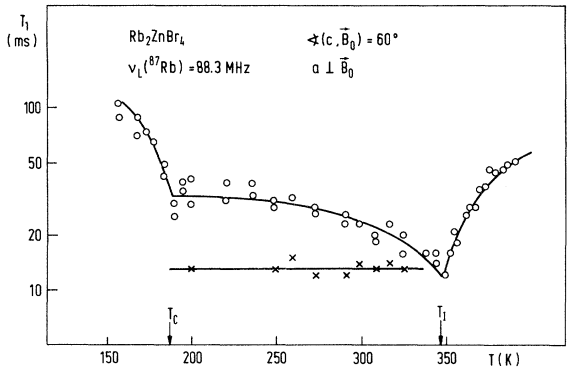

FIG. 8. Temperature dependence of the spin-lattice relaxation time. Circles denote T_1 at the distinct edge singularity, while crosses represent values, obtained in the middle of the frequency distribution in the I phase.

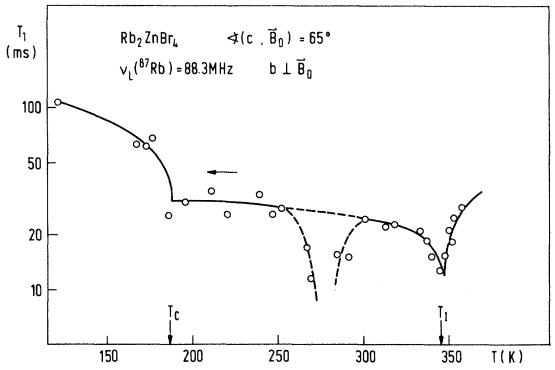

FIG. 9. Temperature dependence of T_1 at a special orientation, where an additional minimum has been observed at $\sim$ 280 K. It is tentatively attributed to the cross relaxation with bromine nuclei.

Rb_2ZnCl_4, the best explanation is cross relaxation with bromine nuclei. Unperturbed ^{81}Br NQR frequencies lie between 55 and 70 MHz,[38] and together with Zeeman interaction the level crossing with $\nu_L(^{87}Rb) = 88.3$ MHz can be fulfilled at special orientations.

VIII. CONCLUSIONS

The above results show the following.

(i) The incommensurate modulation in Rb_2ZnBr_4 can be over most of the I phase described by the "broad soliton," or what amounts to the same, the "plane-wave" limit as the soliton width is large compared to the intersoliton distance.

(ii) Close to T_c the intersoliton distance becomes large as compared to the soliton width and the soliton density vanishes as $T \rightarrow T_c^+$.

(iii) The critical exponent for the amplitude of the order parameter is $\beta - 0.35 \pm 0.03$.

(iv) The spin-lattice relaxation rate has been found to be dominated by phasons at the center of the incommensurate frequency distribution and by amplitudons at the points of extreme nuclear displacements.

(v) Whereas the above results are analogous to what has been found in Rb_2ZnCl_4 the appearance of paraelectric lines is the I phase and the soliton pinning effects together with the sample dependence of T_I and T_c are tentatively attributed to the influence of defects on the properties of the Rb_2ZnBr_4 samples grown in the I phase. These effects have not been observed in Rb_2ZnCl_4 where the sample was grown in the P phase.

ACKNOWLEDGMENT

The authors would like to acknowledge the help of I. P. Aleksandrova in the initial stages of this work.

---

*On leave of absence from Nuclear Research Center "Demokritos" Aghia Paraskevi Attikis, Athens, Greece.

[1]For a review see R. Pynn, Nature (London) 281, 433 (1979), and references therein.

[2]M. Iizumi, J. D. Axe, G. Shirane, and K. Shimaoka, Phys. Rev. B 15, 4392 (1977).

[3]H. Jacobi, Z. Kristallogr. Kristallogeom. Krystallphs. Kristallchem. 135, 467 (1972).

[4]C. J. de Pater and C. van Dijk, Phys. Rev. B 18, 1281 (1978).

[5]K. Gesi and M. Iizumi, J. Phys. Soc. Jpn. 45, 1777 (1978).

[6]M. Takashige, T. Nakamura, M. Udagawa, S. Kojima, S. Hirotsu, and S. Sawada, J. Phys. Soc. Jpn. 48, 150 (1980).

[7]W. L. McMillan, Phys. Rev. B 12, 1187 (1975); 14, 1496 (1976).

[8]D. E. Moncton, J. D. Axe, and F. J. DiSalvo, Phys. Rev. Lett. 34, 734 (1975); Phys. Rev. B 16, 801 (1977).

[9]A. K. Moskalev, I. A. Belobrova, and I. P. Aleksandrova, Fiz. Tverd. Tela (Leningrad) 20, 3288 (1978); I. P. Aleksandrova, A. K. Moskalev, and I. A. Belobrova, J. Phys. Soc. Jpn. 49, Suppl. B, 86 (1980).

[10]F. Milia, Phys. Lett. 70A, 218 (1979).

[11]R. Osredkar, S. Južnič, V. Rutar, J. Seliger, and R. Blinc, Ferroelectrics 24, 147 (1980).

[12]R. Blinc, V. Rutar, J. Seliger, S. Žumer, Th. Rasing, and I. P. Aleksandrova, Solid State Commun. 34, 895 (1980).

[13]B. H. Suits, S. Couturié, and C. P. Slichter, Phys. Rev. Lett. 45, 194 (1980); Phys. Rev. B 23, 5142 (1981). See also C. Berthier, D. Jerome, and P. Molinié, J. Phys. C 11, 797 (1978).

[14]K. Tsuchida, S. Imaizumi, R. Abe, and I. Suzuki, J. Phys. Soc. Jpn. 50, 159 (1981).

[15]R. Blinc, V. Rutar, B. Topič, F. Milia, I. P. Aleksandrova, A. S. Chaves, and R. Gazzinelli, Phys. Rev. Lett. 46, 1406 (1981).

[16]F. Milia and V. Rutar, Phys. Rev. B 23, 6061 (1981).

[17]W. Rehwald and A. Vonlanthen, Solid State Commun. 38, 209 (1981).

[18]R. Blinc, S. Južnič, V. Rutar, J. Seliger, and S. Žumer, Phys. Rev. Lett. 44, 609 (1980).

[19]V. Rutar, J. Seliger, B. Topič, R. Blinc, and I. P. Aleksandrova, Phys. Rev. B 24, 2397 (1981).

[20]G. M. Volkoff, Can. J. Phys. 31, 820 (1953).

[21]C. J. de Pater, Acta Crystallogr. Sect. B 35, 199 (1979).

[22]T. Nakamura, M. Kasahara, and I. Tatsuzaki, J. Phys. Soc. Jpn. 49, 1429 (1980).

[23]C. J. de Pater, Ph.D. thesis, University of Delft, 1980 (unpublished).

[24]K. Gesi and M. Iizumi, J. Phys. Soc. Jpn. 46, 697 (1979); A. Lopez-Echarri, M. J. Tello, P. Gili, E. H. Bocanegra, and J. Fernandez, Ferroelectrics 26, 695 (1980).

[25]M. Pezeril, J. Emery, and J. C. Fayet, J. Phys. (Paris) Lett. 41, L-499 (1980).

[26]T. Matsuda and I. Hatta, J. Phys. Soc. Jpn. 48, 157 (1980).

[27]R. Blinc, F. Milia, V. Rutar, J. Seliger, B. Topič, S. Žumer, I. P. Aleksandrova, and A. S. Chaves, J. Phys. C (in press).

[28]K. Nakanishi and H. Shiba, J. Phys. Soc. Jpn. 44,

1463 (1978).
[29]T. Natterman, J. Phys. C 13, 1265 (1980).
[30]K. Hamano, Y. Ikeda, T. Fujimoto, K. Ema, and S. Hirotsu, J. Phys. Soc. Jpn. 49, 2278 (1980).
[31]C. J. de Pater, Phys. Status Solidi A 48, 503 (1978).
[32]C. J. de Pater, J. D. Axe, and R. Currat, Phys. Rev. B 19, 4684 (1979).
[33]V. Rutar, J. Slak, I. Mele, and R. Blinc, Ferroelectrics 24, 219 (1980).
[34]R. Blinc, V. Rutar, and F. Milia, Phys. Rev. B 23, 4577 (1981).
[35]R. Blinc and B. Žekš, *Soft Modes in Ferroelectrics and Antiferroelectrics* (North-Holland, Amsterdam, 1974).
[36]A. W. Overhauser, Phys. Rev. B 10, 3173 (1971).
[37]S. Žumer and R. Blinc, J. Phys. C 14, 465 (1981).
[38]J. Pirnat, J. Lužnik, Z. Trontelj, and E. Podreka, Proceedings of the Joint ISMAR-AMPERE International Conference on Magnetic Resonance, Delft, 1980 [Bull. Magn. Resonance 2, 250 (1980)].